

Multiple Steady-State Solutions in a Dividing Wall Column Simulation

Jingsong Zhou, Hendrik A. Kooijman, Ross Taylor*

Clarkson University, Potsdam, New York, USA
 taylor@clarkson.edu

Three steady-state solutions are reported for a simulation of a dividing wall column of fixed configuration and specifications. By varying the specified flowrates in certain ranges, a narrow region is found in which three steady-state solutions occur may be found. Further work is needed to uncover additional examples and to explain why MSS exists in this case.

1. Introduction

The existence of multiple steady states (MSS) in multicomponent distillation has been known for a long time. First reports were from analytical or simulation-based studies (see, e.g. Bekiaris et al., 1993; Güttinger & Morari, 1996 for nearly complete historical surveys). To the best of our knowledge the earliest *documented* case of MSS in *multicomponent* distillation can be found in the Ph.D. thesis of C.F. Shewchuk (1974) who found two different solutions for ethanol dehydration using benzene (a system frequently used in later studies of MSS). A later paper by Magnussen et al. (1979) – erroneously said by many others to be the first report of MSS in *multicomponent* distillation – found three steady-state solutions for the same system. It was, however, the Magnussen paper that led to increased interest in MSS with many subsequent publications reporting the occurrence of MSS in different systems, or with different specifications, proposing explanations of why MSS exist, and, relatively recently, experimental studies that confirm that MSS is not a phenomenon that arises solely from the nature of our mathematical models (see, e.g. Müller & Marquardt, 1997; Güttinger et al., 1997). One of the findings of some of the many studies on MSS is that interlinked column systems can exhibit multiplicity, an observation that may lie behind the results reported in this paper.

Wayburn, Seader, and coworkers (see Wayburn and Seader, 1984; Chavez et al., 1986; Lin et al., 1987) used a differential arc length homotopy continuation method and found MSS for the well-known Petlyuk column configuration. A simple DWC is structurally equivalent in some ways at least to a Petlyuk column. Thus, it could, perhaps, be anticipated that a DWC can exhibit multiple steady states. However, the MSS reported in the works of Wayburn, Seader and colleagues, who specified product purities, is what others refer to as input multiplicity, meaning that two or more independent sets of input variables result in the same output condition (see, e.g., Jacobsen and Skogestad, 1991). It is, therefore, unlikely that a real DWC with a fixed wall could exhibit that type of multiplicity (a fixed wall implies that operating specifications should remain more or less the same for each steady state). Output multiplicity is when a single set of input specifications leads to multiple independent sets of outputs; it is an example of that type of multiplicity for a DWC that we report in this paper.

2. Case study

The simulation described here was carried out using an equation-oriented equilibrium-stage parallel column model (PCM) that can be applied to model dividing wall columns (Zhou et al., 2018). In other words, the simulation code uses Newton's method to solve simultaneously all of the model equations. One of the advantages of an equation-based approach is that it becomes very easy to include in the model heat transfer across the wall. Accounting for heat transfer across the wall is not straightforward in the more widely used approach in which a DWC is modelled using a multi-column model in a sequential-modular simulator.

Complete details of the parallel column model, the solution procedure, and the initialization (which is of some importance here) are given by Zhou et al. (2018).

The example that exhibits multiple steady states is derived from a comprehensive experimental study conducted by Roach (2017) at the University of Texas at Austin.

The pilot DWC at the University of Texas, Austin, uses Sulzer Mellapak 500Y with an HETP of 9.5 inches/stage (as indicated by Sulzer). The welded dividing wall (1/4 inch 304 SS) divides the cross sectional area exactly in half.

The DWC is simulated with 38 equilibrium stages in total, with condenser and reboiler included in that number (this is the same number of stages used by Roach in her simulations). Figure 1b shows the diagram of the DWC with the stage numbers we use in our parallel column model. The feed enters on stage 14, and the liquid side product is taken from stage 25. Specifications for our simulation are provided in Table 1 (at the end of the paper); the case study is adapted from experiment A9ii in the dissertation of Roach (2017). The important specification that differs from her experimental values is the reflux ratio, 12 here instead of 6.

The NRTL activity model is used to model vapour liquid equilibrium, with parameters obtained from Appendix D of Roach's dissertation. Vapour pressures are estimated using the correlation in ChemSep (All column simulations were carried out using the parallel column model in ChemSep (www.chemsep.com)).

Table 1: Specifications for Dividing Wall Column Simulation

Base Case Number in Roach (2017)	A9ii		
Feed flowrate (lb/h)	51.57	Shell heat transfer coefficient (W/m ² K)	14
Feed state	Saturated**	Wall heat transfer coefficient (W/m ² K)	1600***
Feed Composition (wt%)		Surroundings temperature (°F)	75.75
1-Hexanol	7.6		
1-Octanol	74.6	Sidedraw rate (lb/h)	38.72
1-Decanol	17.8	Bottoms flow rate (lb/h)	8.99
Pressure overhead (psia)	0.90	Overhead reflux ratio	12*
Overall pressure drop (in H ₂ O)	2.41		
Wall region pressure drop (in H ₂ O)	1.09	Vapour split (left % / right %)	50 / 50
		Liquid split (left % / right %)	26 / 74

* Actual value in experiment of Roach (2017) was 6
 ** Actual feed in the experiment was not saturated
 *** See discussion

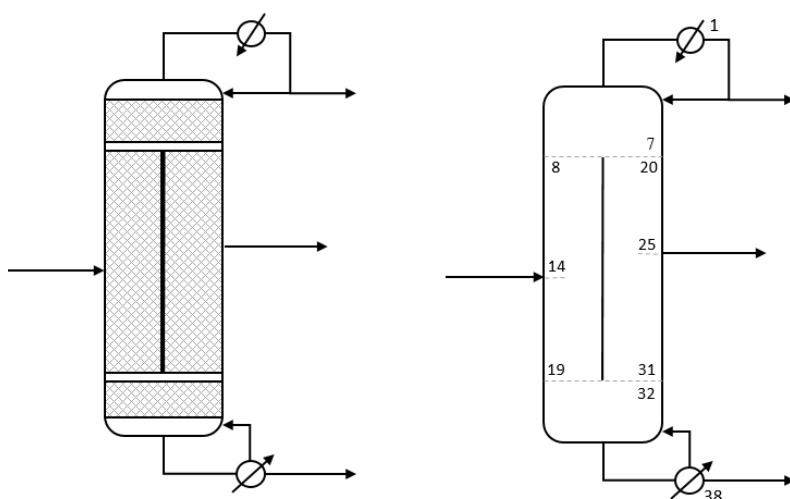


Figure 1: (a) Diagram of the packed DWC; (b) Diagram of the DWC with numbers indicating stages in model.

Three steady state solutions to this simulation problem are summarized in Table 2 and in Figures 2–3. Figure 2 shows temperature profiles of three steady state solutions to the simulation in Table 1; Figure 3 shows the flowrate and liquid mole fraction profiles for the three steady state solutions.

Table 2: Summary of Multiple Steady State Solutions

	Solution 1			Solution 2			Solution 3		
	Top	Side	Bottom	Top	Side	Bottom	Top	Side	Bottom
Recovery (%) *	98.1	99.7	97.9	98.3	99.9	97.9	98.5	99.7	96.7
Condenser duty (Btu/h)	-11589			-11583			-11586		
Reboiler duty (Btu/h)	24645			24478			23587		
Flowrates (lbmol/hr)									
from reboiler	0.90642			0.90018			0.86056		
to condenser	0.49069			0.49093			0.49111		

* 1-hexanol in top product, 1-octanol in side draw, 1-decanol in bottom product

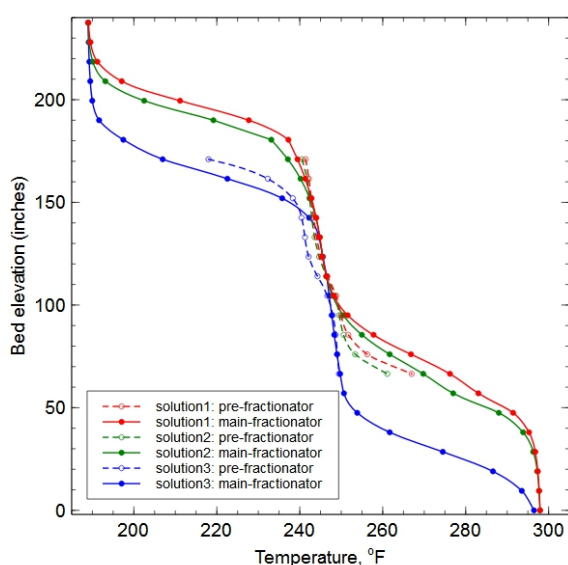


Figure 2: Temperature profiles of three steady-state solutions.

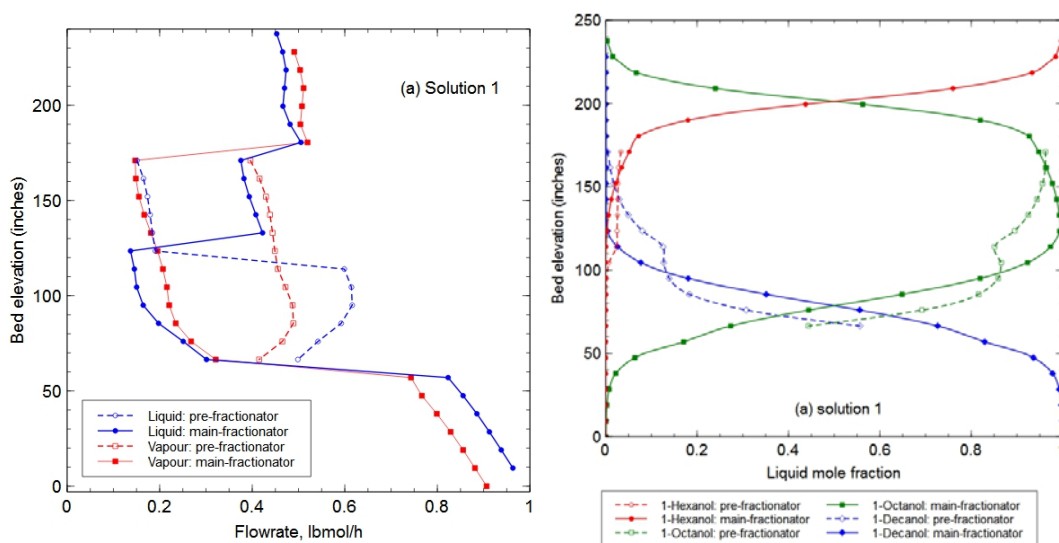


Figure 3: Flowrate and liquid phase mole fraction profiles for three steady-state solutions for the Dividing Wall Column in Table 1 (continue)

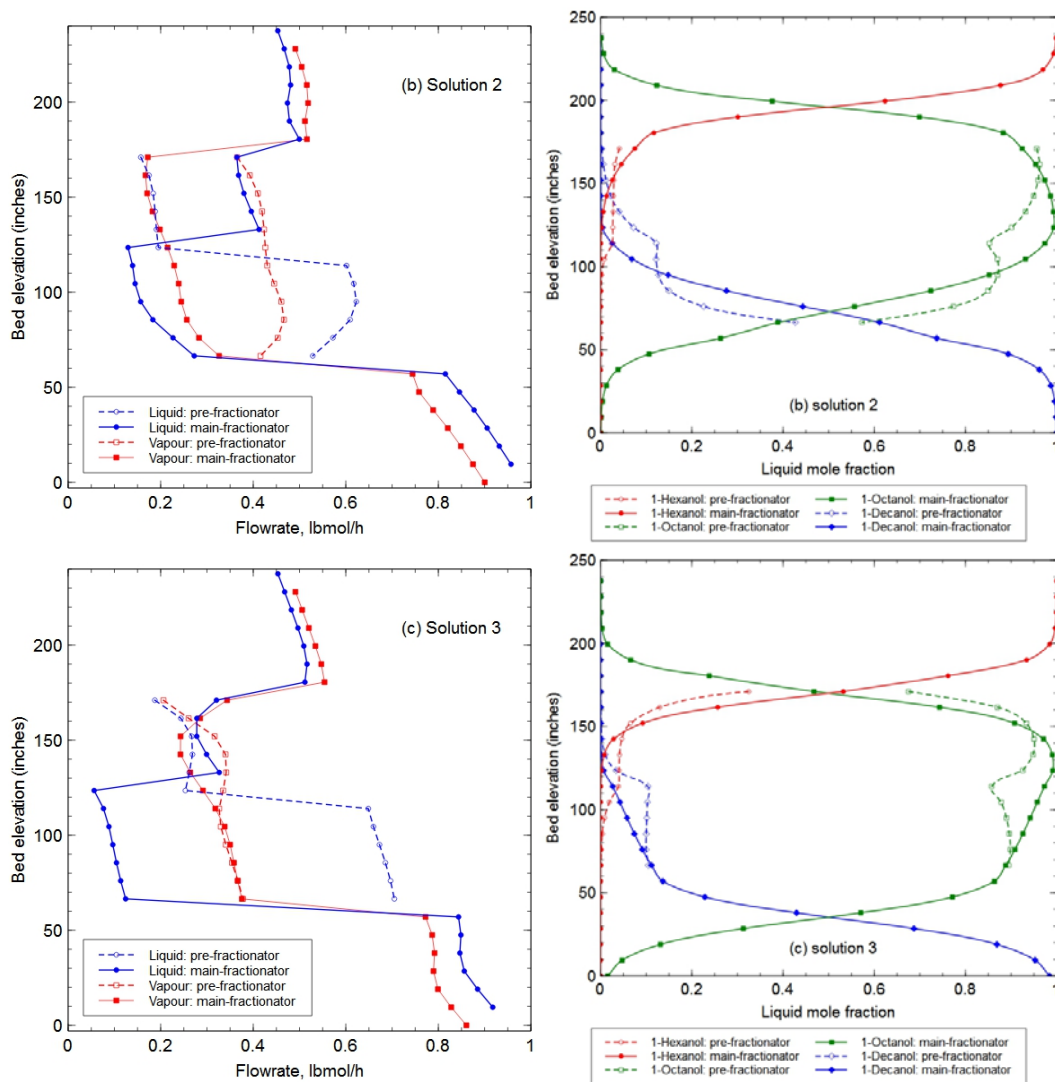


Figure 3: Flowrate and liquid phase mole fraction profiles for three steady-state solutions for the Dividing Wall Column in Table 1.

To gain further insight, we varied the side product mass flowrate from 38.68 lb/h to 38.75 lb/h, while retaining the bottom flowrate at 8.99 lb/h. The effect of varying the side product mass flowrate on the top and middle product purities is shown in Figure 4, with an s-shape curve (for the top product purity) and a bow-tie shape (for the middle product purity) shown in the plots. It is worth noting that the curves in Figure 4 should be continuous in the range of varying side product flowrate, although the curves are not closed at the connections of different solutions due to the extreme difficulty of obtaining convergence of the simulation in the close vicinity of the turning points. It can be concluded from the plots that three steady-state solutions exist if the side product flowrate is in the very narrow range of 38.702 lb/h to 38.724 lb/h. If the side product flowrate is less than 38.702 lb/h, only solution 1 exists; if the side product flowrate is greater than 38.724 lb/h, solution 3 is the only one.

These MSS do not disappear when the vapour split below the wall is other than 50% / 50% as, following the experimental work of Roach (2017), specified in the simulations reported here.

Not shown are (because they are not sufficiently different) are similar plots that show the multiplicity as a function of the bottom and side flow rates expressed in molar units, rather than mass units. Thus, that the existence of multiple steady-state solutions is due to mass flow specifications when the model equations employ molar flows, advanced by Jacobsen and Skogestad (1991) as a potential explanation for MSS in some distillation systems, seems unlikely here.

Figure 5 shows the result of varying both side draw and bottoms rate at the same time. The side product flowrate is varied over the same range as before, and bottom product flowrate varied from 8.96 lb/h to 9.03 lb/h. At each combination of side draw rate and bottoms rate the simulation is run from 3 different starting points; the results used to create the surface plots in Figure 5. These figures show a three-dimensional s-shaped surface corresponding to the curve in Figure 4a and a bow-tie surface corresponding to the curve in Figure 4b.

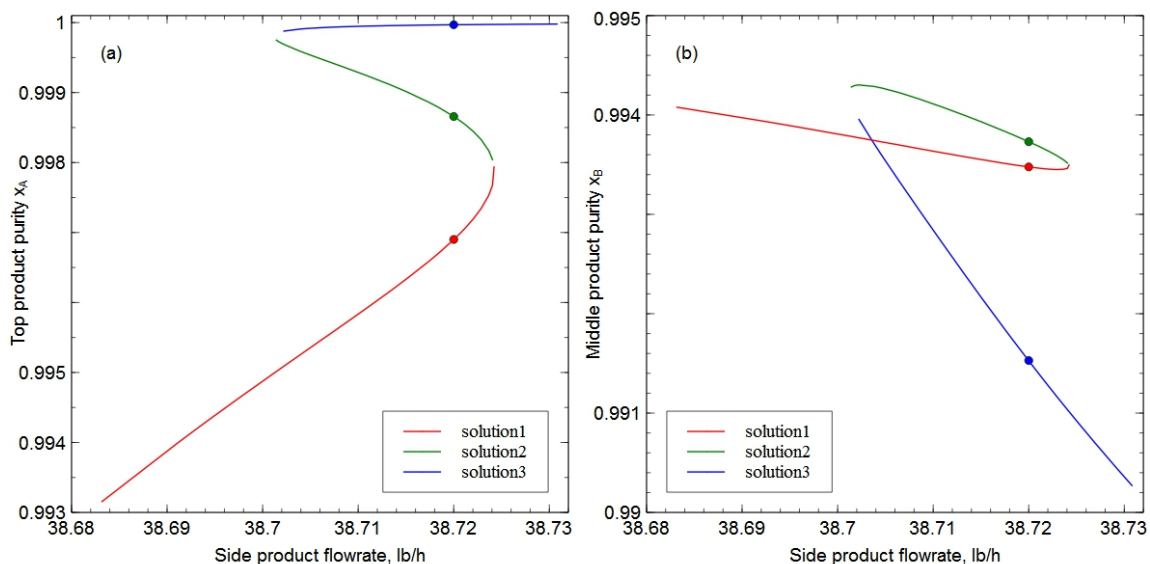


Figure 4: Product purity as a function of side product mass flowrates: (a) top product purity, and (b) middle product purity vs. side product mass flowrate. Points represent the solutions shown in Figures 2 and 3.

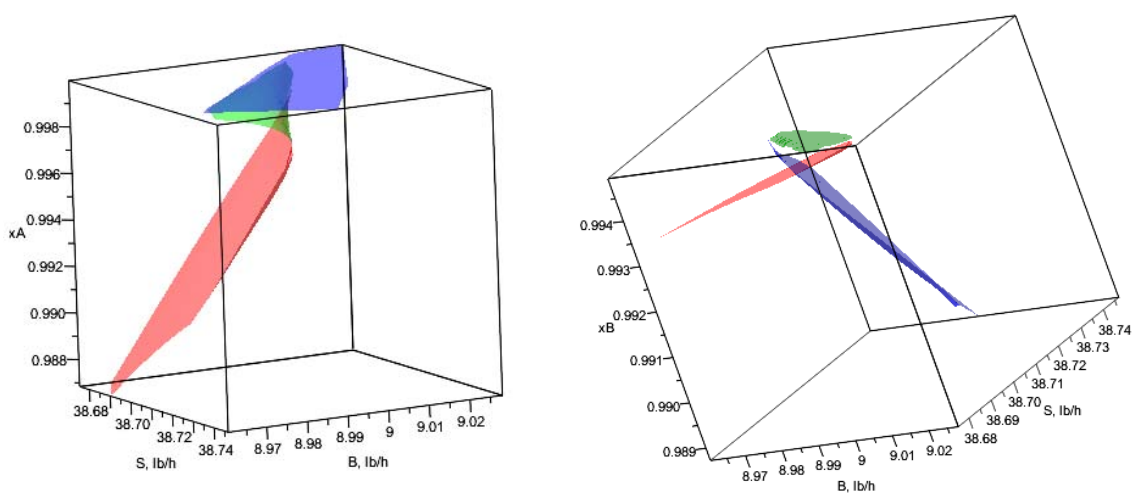


Figure 5: Multiple steady-state solutions obtained when varying side product and bottom product flowrates simultaneously: (a) Purity of main compound in the distillate (left), and (b) mole fraction of main product in the sidestream. B = Bottoms mass flow, S = sidestream rate (both in lb/h – the units used in Roach, 2017).

3. Discussion

Our discovery of multiple steady state solutions shown above came about entirely by accident. We were experimenting with different ways to initialize the flow rates, temperatures, and mole fractions in the parallel column model and obtained different solutions depending on what particular method was used for the initialization.

In the example shown here the window for MSS is quite narrow and is somewhat sensitive to the value of the wall heat transfer coefficient. For this simulation we used a value at the upper end of the range indicated by Roach (2017) (she quotes values of the wall heat transfer coefficient from 14 to more than 1800 W/m²K, with one very high value for about 30,000 W/m²K). We were not able to find MSS for this particular simulation when heat transfer across the wall was ignored. This might mean that these MSS are dependent on wall heat transfer; it may, instead, mean that the window for MSS has moved to a location we were not able to find.

Given the large number of more or less conventional distillation processes already demonstrated to show MSS, we speculate that it is likely that there are many other DWC operations that exhibit multiplicity. However, we have not yet been able routinely to find MSS in other DWC systems. It is possible that MSS in other cases will be hard for others to find because the vast majority of DWC simulations are carried out with multi-column models in commercial sequential modular simulation systems in which it is not straightforward to include heat transfer. (It is not, however, impossible to do so, as evidenced by the work of Roach). In addition, it is not easy to exercise any control over the computational process in a commercial simulation program. It is very easy to include heat transfer in the PCM used in this work (Zhou et al., 2018). What may help here is to couple the PCM to an arc length continuation method that can assist with the automatic location of MSS in DWCs (see, for example, the works of Wayburn, Seader and coworkers cited in the introduction).

4. Conclusion

Multiple steady-state solutions are found in simulations of a DWC with two product flowrates specified in mass units. Variation of both specified mass flowrates result in a narrow region where three solutions exist. The reasons underlying multiplicity in the DWC model remain unclear. Possible factors that may cause multiple steady-state solutions include heat transfer across the dividing wall, heat loss to the surroundings, fixed vapour and liquid traffic on both sides of the dividing wall, and more. Further investigation is needed to gain deeper understanding of the multiplicity in modelling DWCs. Such investigation might be helped considerably by using differential arc-length continuation.

Given that multiplicity has been verified experimentally in simple distillation columns we suspect that it is only a matter of time before the experimental verification of MSS in a real DWC is confirmed.

References

- Bekiaris N., Meski G.A., Radu C.M., Morari M., 1993, Multiple steady states in homogeneous azeotropic distillation, *Industrial & Engineering Chemistry Research*, 32 (9), pp. 2023-2038
- Chavez C R., Seader J.D., Wayburn T.L., 1986, Multiple steady-state solutions for interlinked separation systems, *Industrial & engineering chemistry fundamentals*, 25(4), 566-576.
- Güttinger T.E., Dorn C., Morari M., 1997, Experimental Study of Multiple Steady States in Homogeneous Azeotropic Distillation, *Industrial & Engineering Chemistry Research*, 36 (3), pp. 794-802
- Güttinger T.E., Morari M., 1996, Multiple Steady States in Homogeneous Separation Sequences, *Industrial & Engineering Chemistry Research*, 35 (12), pp. 4597-4611
- Jacobsen E.W., Skogestad S., 1991, Multiple steady states in ideal two-product distillation, *AIChE Journal*, 37(4), 499-511.
- Lin W.J., Seader J.D., Wayburn T.L., 1987, Computing multiple solutions to systems of interlinked separation columns, *AIChE Journal*, 33(6), 886-897.
- Magnussen T., Michelsen M.L., Fredenslund A., 1979, Azeotropic distillation using UNIFAC, *Inst. Chem. Eng. Symp. Ser.*, Vol. 56, no. 44.2, pp. 1-4.
- Müller D., Marquardt W., 1997, Experimental Verification of Multiple Steady States in Heterogeneous Azeotropic Distillation, *Industrial & Engineering Chemistry Research*, 36 (12), pp. 5410-5418
- Roach B.J., 2017, A design model for dividing wall distillation columns, PhD Thesis, University of Texas at Austin, Texas, USA.
- Shewchuk C.F. 1974, Computation of Multiple Distillation Towers, Ph.D. Thesis, University of Cambridge.
- Wayburn T.L., Seader J.D., 1984, Solution of systems of interlinked distillation columns by differential homotopy-continuation methods, In *Proceedings of the Second International Conference on Foundations of Computer-Aided Process Design*, pp. 765-862. CACHE Ann Arbor.
- Zhou J., Kooijman H., Taylor R., 2018, Parallel column model for dividing wall column simulations, Paper in preparation.